Computation of Aero-Optical Distortions over a Cylindrical Turret with Passive Flow Control

Kan Wang* , Meng Wang† , Stanislav Gordeyev‡ and Eric Jumper§
University of Notre Dame, Notre Dame, IN 46556

Large-eddy simulations are performed for compressible flow over a cylindrical turret with a flat optical window, with and without passive control in the upstream boundary layer. Statistics of the flow field and optical distortions are computed and compared with experimental measurements. Results show reasonable agreement with experimental data for the baseline case without control. When passive control is applied using thin and tall pins, the numerical results confirm key experimental findings, although some quantitative discrepancies are observed. The flow simulated is characterized by two distinct shear layers above the optical window, whose combined effect leads to slightly reduced optical distortions compared to the uncontrolled flow with a single strong shear layer.

I. Introduction

Aero-optical distortions caused by density variations in a compressible flow adjacent to an optical turret are detrimental to airborne laser systems. Many experimental, analytical and numerical investigations have been conducted in order to understand and mitigate these effects.[1] In recent years, large-eddy simulation (LES) has emerged as a tool for studying aero-optics because of its ability to capture a broad range of turbulence scales relevant to optical aberrations. A number of canonical flow problems including, for example, flat-plate turbulent boundary layers,[2,3] turbulent free shear layers[4,5] and flow over a circular cylinder[6,7] have been simulated by LES, and optical distortions caused by these flows have been investigated. Optical aberrations by more practical flows such as flow over a fuselage/turret configuration[8] have also been considered. Despite these efforts, accurate predictions of flow-induced optical aberrations remain a significant challenge, particularly for realistic complex geometries and at high Reynolds numbers.

A cylindrical turret with a flat window mounted on two flat surfaces of different altitudes has been used as a simplified model of optical turrets in recent experiments,[9–11] and its aerodynamic and aero-optical characteristics have been investigated. In addition to measuring the optical distortions caused by the separated shear layer over the cylindrical turret, Gordeyev et al.[10] investigated the use of passive control devices placed on the upstream surface for mitigating the optical effects. They considered small disturbance devices, including small pins and vortex generators, as well as relatively large disturbance devices mainly consisting of large vortex generators. It was found that small disturbance devices were able to improve the optical-propagation environment in the range of elevation angles from 97° to 105° but had almost no effect beyond 110°, while the large disturbance devices increased the distortions at all angles up to 140°. In this study, pins of different diameters were tested but the heights remained the same, which was 71% of the boundary layer thickness.

More parametric studies were performed recently[11] to improve the optical environment over the window at large elevation angles over which flow separation cannot be prevented. The pin height was varied between 1.2 and 3.2 times the boundary layer thickness δ, or 0.12 and 0.31 times the cylindrical turret radius R, which is 2 inches. The pin diameter was varied between $0.01R$ and $0.04R$, and pins spacing was varied between $0.05R$ and $0.1R$. Velocity profiles measured for "tall pins" with height of $0.28R$ (2.8δ), diameter of $0.02R$

*Graduate Student, Department of Aerospace and Mechanical Engineering, Student Member AIAA.
†Associate Professor, Department of Aerospace and Mechanical Engineering, Senior Member AIAA.
‡Research Associate Professor, Department of Aerospace and Mechanical Engineering, Senior Member AIAA.
§Professor, Department of Aerospace and Mechanical Engineering, Fellow AIAA.

and spacing of $0.05R$ (Configuration C in Ref. 11) showed that the pins generated a strong second shear layer from the top of the pins, and reduced the turbulence intensity in the main shear layer significantly above the optical window. Velocity profiles for the case of smaller-diameter pins with height of $0.31R$ (3.2δ), diameter of $0.01R$ and spacing of $0.05R$ (Configuration F in Ref. 11) showed a weaker second shear layer which had less interaction with the main shear layer compared to Configuration C and thus caused less reduction in turbulence intensity in the main shear layer. Optical distortions depend on the turbulence levels in both shear layers. Measurements showed that configuration C did not reduce optical distortions except for elevation angle of 150°. Configuration F improved the aero-optical environment by 15–20% for the range of elevation angles between 120° and 145°. Other pin configurations examined were not very effective. A simple model was proposed to explain the flow-control effectiveness for the aero-optical reduction.

Motivated by the need for accurate aero-optical predictions and inspired by the experiment of Gordeyev et al.,[10] Wang and Wang[12] carried out LES to study the aero-optical distortions caused by a Mach 0.5 turbulent boundary layer flow over a cylindrical turret as in the experiment. The elevation angle was fixed at 120° in the simulation. Results showed that the root-mean-square of optical path difference (OPD_{rms}) caused by the separated shear layer was five times as large as that caused by the attached boundary layer upstream of the turret. The predicted OPD_{rms} was in good agreement with experimental values despite much reduced Reynolds number in their simulation, suggesting relative insensitivity to the Reynolds number.

More recently, Morgan and Visbal[13] performed simulations of flow over a cylindrical turret at three elevation angles (90°, 100° and 120°) using high-order implicit large eddy simulation (ILES). Reasonable solutions were shown by comparison with mean and fluctuating velocity profiles from experimental data. A passive control study was conducted for the 100° case. A row of pins with diameter $0.06R$, height $0.1R$, and spacing $0.12R$ were placed $1.0R$ upstream of the turret. The counter-rotating streamwise vortices in the upper portion of the pin wake energized the boundary layer and decreased the size of separation bubble by 56% compared to the baseline case. Although optical distortions were not calculated, turbulent kinetic energy levels were reduced over the optical window, indicating that the pins may improve the aero-optical environment.

The present study is focused on using LES to predict the effects of cylindrical pins as passive control devices on mitigating the optical aberrations by flow over a cylindrical turret. The long-term objectives are to establish and validate a computational framework, study the physical mechanisms of passive control, and investigate the dependence on pin parameters together with ongoing experiments.[11] In this paper,simulation results are presented for a baseline case without passive control and a case with pins as passive control devices at an elevation angle of 120°. The baseline case is the same as first presented in Ref. 12 but is recomputed with a longer computational domain to better accommodate the large separation bubble behind the turret. It is presented briefly here to compare with experimental data and serve as a reference to evaluate the control effect. The controlled case corresponds to Configuration C in Gordeyev et al.[11] It is simulated to assess the feasibility and accuracy of the LES approach and study mechanisms for aero-optical mitigation.

II. Numerical Approach

In the aero-optical computation, LES is conducted to provide a detailed description of the turbulent flow field, especially the fluctuating density field. The optical index of refraction is obtained from fluctuating density field through the Gladstone-Dale relation,[15] and a simple ray tracing calculation is performed to compute the optical wavefront distortions.

II.A. Flow Simulation

The flow-field simulation is performed using an unstructured-mesh compressible LES code developed at the Center for Turbulence Research, Stanford University.[14] The code solves the spatially filtered compressible Navier-Stokes equations in conservative form with the state equation using low-dissipative, robust numerical algorithms. It employs a second-order finite volume scheme for spatial discretization and a hybrid implicit/explicit Runge-Kutta scheme for efficient and stable time advancement. The effect of subgrid-scale motions is modeled using the dynamic Smagorinsky model. This code is parallelized with MPI and achieves very high parallel efficiency.

The computational set-up is shown schematically in figure 1. In the experiment of Gordeyev et al.,[11] the flat window and the cylinder can be rotated to position the laser beam relative to the freestream at any angle

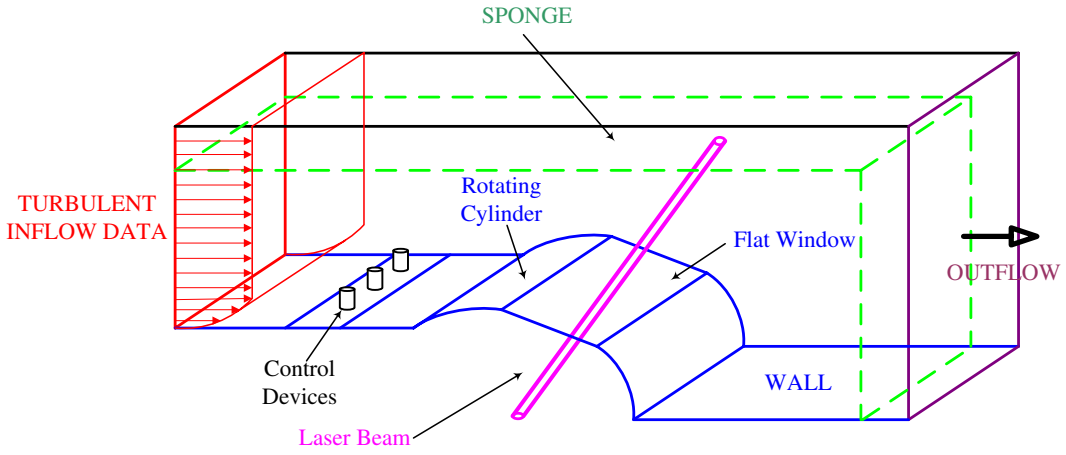

Figure 1. Computational set-up for flow over a cylindrical turret with a flat window and flow-control devices.

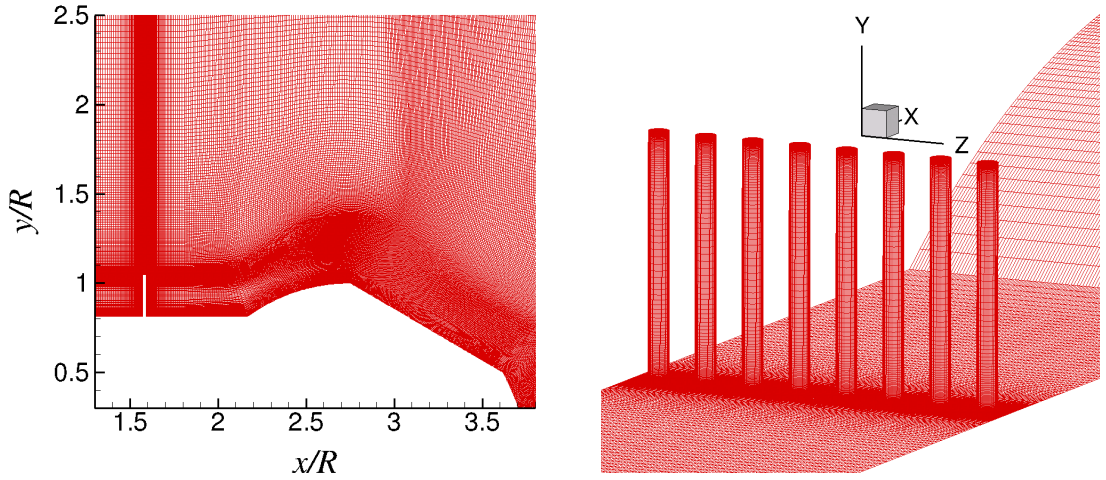

(a) (b)

Figure 2. Computational mesh for flow over a cylindrical turret with tall pins: (a) A spanwise cut through the center of a pin; (b) Surface mesh around the pins.

between 90° and 150°. This angle is fixed at 120° in the present simulation. The computational domain size based on the radius R of the cylinder is $12.3R$, $2.81R$ and $0.39R$ in the streamwise (x), wall normal (y) and spanwise (z) directions, respectively. The center of turret is located at $x = 2.75R$. In the case with passive control, small pins of diameter $0.02R$ and height $0.24R$ are placed at a distance $1.1675R$ upstream of the turret center. The separation between neighboring pins is $0.05R$, and eight pins are included in the computational domain in spanwise direction. The Reynolds number in the simulation is $Re_R = 8.8 \times 10^4$, which is 15% of the experimental value to make the LES affordable. There is evidence[12] that with turbulent separation, the free shear layer above the optical window and the induced optical distortions are not sensitive to Reynolds number. The turbulent boundary layer at the inlet has a thickness of $0.13R$, and the corresponding Reynolds number based on momentum thickness is $Re_\theta = 1400$.

Introducing pins into the flow configuration poses significant computational challenges, as they create energetic small-scale structures. The simulation must capture the interaction of these structures with incoming turbulent eddies with high fidelity. In addition, the pins present a geometric complexity which affects grid quality. In the present simulation, the computational mesh is carefully designed to promote solution stability and accuracy.

The computational mesh is shown in figure 2(a) in a spanwise cut and figure 2(b) on a portion of the

surface including the pins. The mesh is refined near the separation point at the upper corner of the flat window and along the separated shear layer, and stretched gradually towards the top and outlet boundaries. Grid points are also clustered around the pins to provide resolution of the flow structures generated by the pins. Grid quality in terms of stretching and skewness are carefully controlled as required by the low-dissipative numerical scheme. In total, 11 million computational cells are employed for the baseline simulation, and 26 million cells are employed for the controlled case.

The time-dependent turbulent inflow data are generated by an auxiliary simulation of a flat-plate turbulent boundary layer adopting an extension of the rescale and recycle technique of Lund et al.[16] to compressible flows.[17,18] The boundary conditions for top and outflow boundaries are dirichlet. A sponge layer with thickness of $0.5R$ is applied along these two boundaries to implement a non-reflecting boundary condition.[19] In the sponge region, the flow structures and acoustic waves are damped out, and flow quantities are forced to prescribed reference values obtained from a RANS simulation. Periodic boundary conditions are imposed in the spanwise direction. The boundary conditions for the bottom wall are no-slip, no penetration and adiabatic.

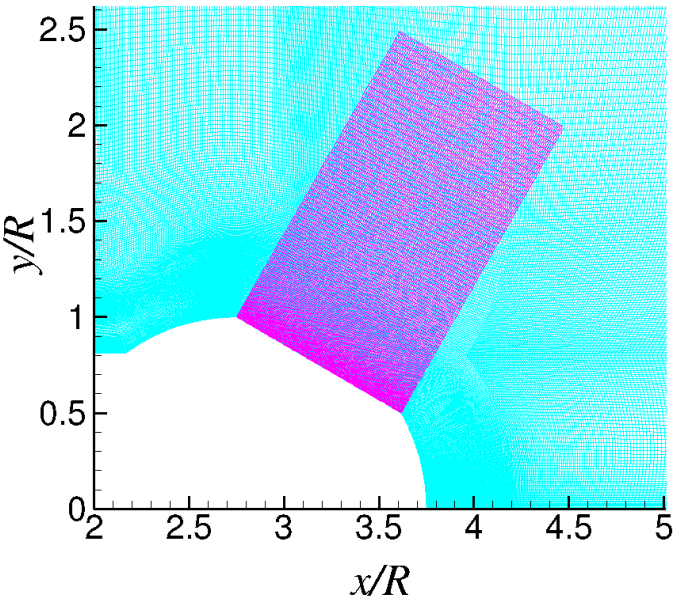

Figure 3. Two grids in an x-y plane for the cylindrical-turret aero-optical simulations: an unstructured mesh (light blue) for flow simulation and a Cartesian mesh (purple) for optical calculation.

II.B. Optical Computation

The refractive index is related to density by the Gladstone-Dale law[15]

$$n - 1 = K_{GD}\rho, \tag{1}$$

where K_{GD} is the Gladstone-Dale constant. The optical path length (OPL) of a beam is defined as[1,20]

$$OPL(x', y', t) = \int_{z_0'}^{z_1'} n(x', y', z', t)dz', \tag{2}$$

where x', y', and z' are the coordinates for optical calculations, with z' in the direction of propagation and x' and y' in the plane normal to the beam. z_0' and z_1' are boundaries of the turbulence region along the beam path. Wavefront distortions are described by the beam's optical path difference (OPD), which is the variation of OPL about its mean,

$$OPD(x', y', t) = OPL(x', y', t) - \overline{OPL(x', y', t)}, \tag{3}$$

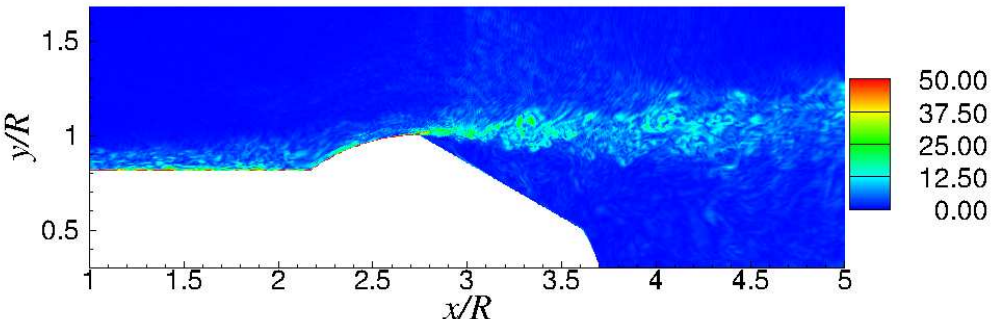

Figure 4. Instantaneous vorticity magnitude $\omega R/c_\infty$ in a spanwise cut in the baseline case.

where the overbar denotes averaging in the x'-y' plane. In practice, $\overline{OPL(x',y',t)}$ is removed along with tip/tilt by a least square surface fitting method. At each time step, parameters A, B and C are determined by minimizing

$$G = \int\int_{Ap} \left[OPL(x',y',t) - (A + Bx' + Cy')\right]^2 \mathrm{d}x'\mathrm{d}y' \tag{4}$$

where Ap denotes the aperture, and then $OPD(x',y',t)$ is computed from

$$OPD(x',y',t) = OPL(x',y',t) - (A + Bx' + Cy'). \tag{5}$$

To compute the optical quantities, a Cartesian beam grid is used to follow the optical path through the turbulence region as shown in figure 3. A linear interpolation scheme is employed to interpolate the density field from the unstructured LES grid onto the beam grid. After the interpolation, the integration in Eq. (2) is carried out to obtain the OPL.

III. Results and Discussion

III.A. Flow Field without Control

An instantaneous flow field for the baseline case is illustrated in figure 4 in term of vorticity magnitude. The figure shows a realistic turbulent boundary layer starting from the inlet and its separation at the upper corner of the flat window, forming a free shear layer behind the turret. The instability of the thin shear layer modulated by the turbulent boundary-layer eddies generates a wide range of scales, which are responsible for optical aberrations.

Profiles of mean velocity and root-mean-sqaure (rms) of velocity fluctuations are plotted in figures 5 and 6, respectively, along with experimental data of Gordeyev et al.[11] at three streamwise locations. These profiles illustrate the evolution of the separated shear layer above the optical window. The simulation results show that in the shear layer the magnitude of velocity fluctuations reaches approximately 20% of the freestream velocity. Compared to the mean velocity profiles from the experiment, the simulation results exhibit a good agreement in terms of the shape and thickness of the shear layer but a small upward shift in the shear layer position. There are some discrepancies in velocity fluctuations as well. The fluctuation levels from the simulation are higher than those in the experiment by up to 25%. The discrepancies may be caused by the boundary conditions or reference values in the sponge region, or the 3-D effect in the experiment which is not considered in the simulation. Overall, the simulation and experiment are in fair agreement.

III.B. Flow Field with Control

Figures 7(a) and 7(b) show the vorticity magnitude and the second invariant of velocity gradient, respectively, at a time instant from the simulation with flow control. Turbulent boundary-layer structures are convected from the inlet and impinge on the pins, which are taller than the boundary layer thickness. New and more intense turbulence structures are generated in the wake of the pins. The interactions between incoming turbulence and wake structures behind the pins have a strong effect on the boundary layer development. In comparison with figure 4, a second shear layer, as discussed by Gordeyev et al.,[11] is clearly observed starting

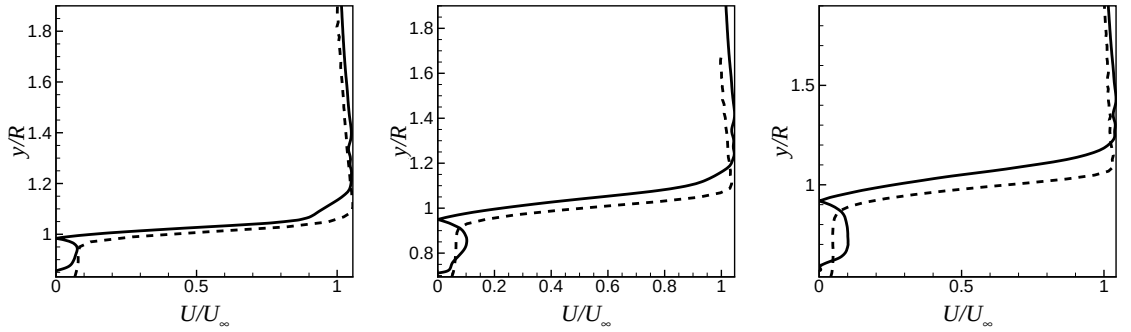

(a) $x = 3.0R$ (b) $x = 3.25R$ (c) $x = 3.5R$

Figure 5. Mean velocity profiles for the baseline case: ———, LES; - - - - -, experiment of Gordeyev et al.[11]

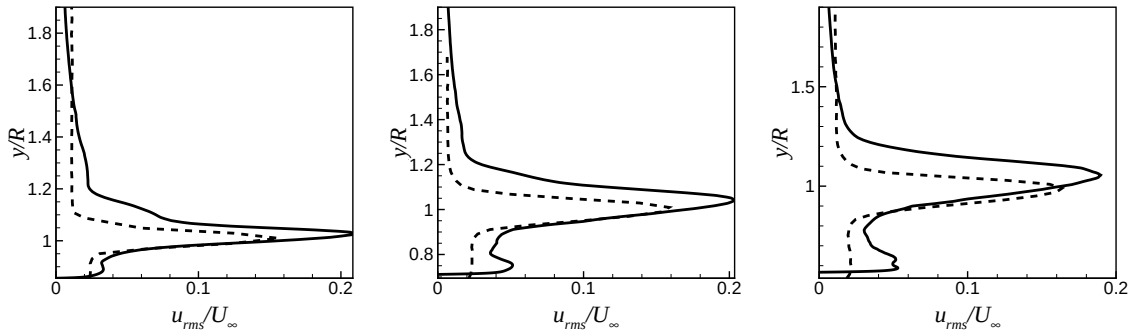

(a) $x = 3.0R$ (b) $x = 3.25R$ (c) $x = 3.5R$

Figure 6. Root-mean-square of velocity fluctuations for the baseline case: ———, LES; - - - - -, experiment of Gordeyev et al.[11]

from the pin top. It is weaker than the main shear layer and grows slowly. The two shear layers remain distinct above the flat window and merge afterwards, resulting in a wider turbulence region compared to the baseline case, which is consistent with experimental observations.[11]

Profiles of mean velocity and rms of velocity fluctuations are shown in figures 8 and 9, respectively, at three streamwise stations above the window. Both numerical and experimental data are plotted for comparison. The numerical solutions capture the major effects of the pins: the presence of the second shear layer introduces a mean velocity deficit above the main shear layer and a second peak in the velocity fluctuation profiles. The turbulence intensity in the main shear layer is reduced by approximately 20% around the center of the optical window ($x = 3.25R$), and the turbulence region is widened at the same time. However, substantial quantitative discrepancies are found between the numerical profiles and experimental data. From the experiment the second shear layer is stronger and the turbulence intensity in the main shear layer is reduced more significantly than their counterparts from the simulation. This is likely caused by insufficient grid resolution in the wake of pins, which causes the second shear layer to lose strength quickly in the downstream direction. The large number of pins and long distance to the optical window make the wake flow extremely expensive to resolve. A careful assessment of the resolution requirement is being conducted to improve agreement with experiment in future simulations. Despite the discrepancies, the current LES results capture the qualitative effect of pins.

Density fluctuation profiles at the same three streamwise stations above the optical window are plotted in figure 10. Peaks from the two shear layers can be clearly observed in the case with pins. Around the center of the flat window, the level of density fluctuations in the main shear layer is reduced by over 1/3 relative to the baseline case, and the magnitude of density fluctuation in the second shear layer reaches 70% of that in the main shear layer. The significant reduction in peak value suggests that a reduction in optical distortions is possible despite the increased width of the turbulence region and the occurrence of the secondary peak.

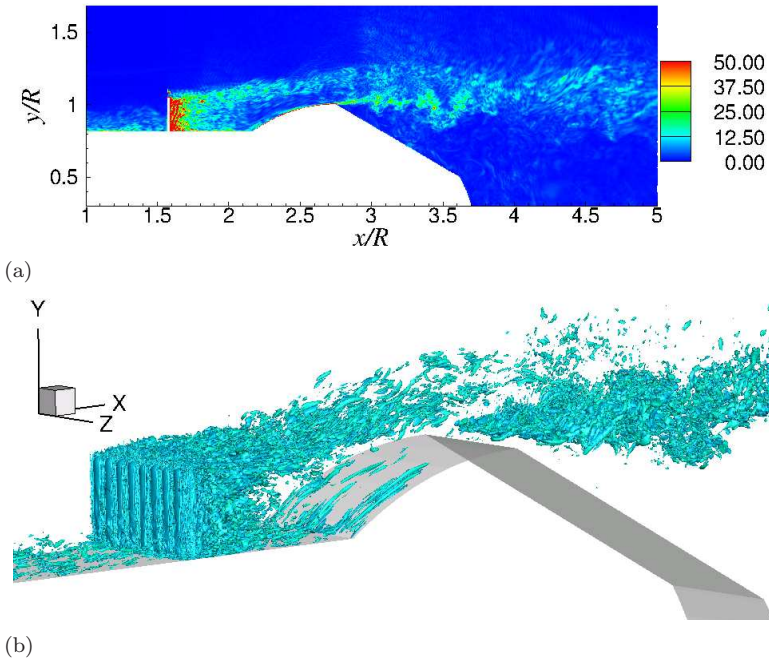

Figure 7. Instantaneous flow field with control devices: (a) Vorticity magnitude $\omega R/c_\infty$ in a spanwise cut through the center of a pin; (b) Iso-surfaces of second invariant of velocity gradient $Q(R/U_\infty)^2 = \pm 200$.

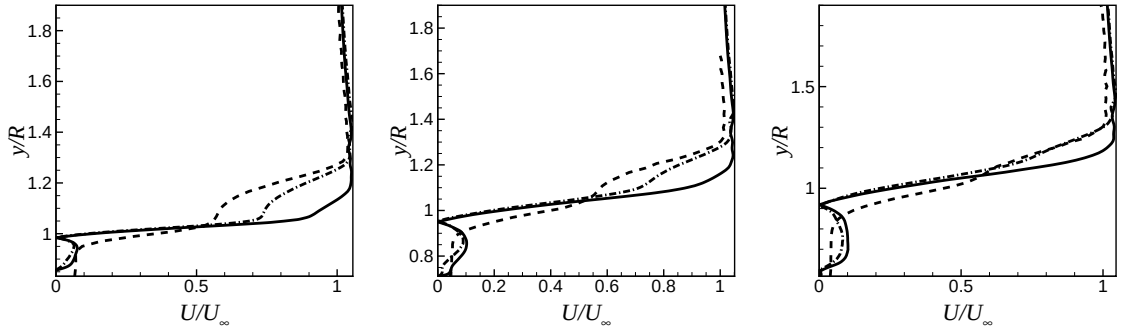

Figure 8. Mean velocity profiles above the flat window with and without pins: ———, LES baseline; – · – · –, LES with passive control; - - - - -, experiment with passive control.[11]

III.C. Optical Results

The distortions of an optical beam of aperture size $0.74R \times 0.39R$ through the center of the flat window are computed. The time-averaged OPD_{rms} induced by the baseline case is $6.79 \times 10^{-7}R$. Based on the dimensions in the experiment, $R = 2$ *in*, and thus the above OPD_{rms} is approximately 0.035 μm. The time-averaged OPD_{rms} induced by the flow with passive control is $6.39 \times 10^{-7}R$, or 0.032 μm, which represents a reduction of 6% over the baseline case. This pin configuration is thus not very effective in improving the aero-optical environment over the turret based on the simulation results.

In the experiment of Gordeyev et al.,[11] the OPD_{rms} for this pin configuration was found to be slightly higher than the baseline value. This is contrary to the simulation result, but it should be noted that the deviation from baseline value is small in both the experimental and numerical results. The difference between numerical and experimental values can be explained by the different turbulence intensity profiles discussed earlier. The experimental data showed two peaks of similar magnitude, whereas the simulation overpredicted the primary peak and underpredicted the peak associated with the second shear layer. In fact. the LES intensity profiles resemble qualitatively the profiles for Configuration F in the experiment, which resulted in

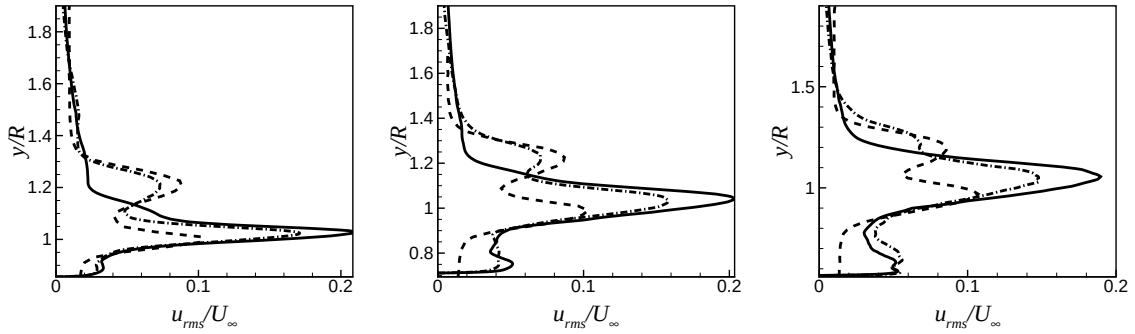

(a) $x = 3.0R$ (b) $x = 3.25R$ (c) $x = 3.5R$

Figure 9. Root-mean-square of velocity fluctuations with and without pins: ———, LES baseline; – · – · –, LES with passive control; - - - - -, experiment with passive control.[11]

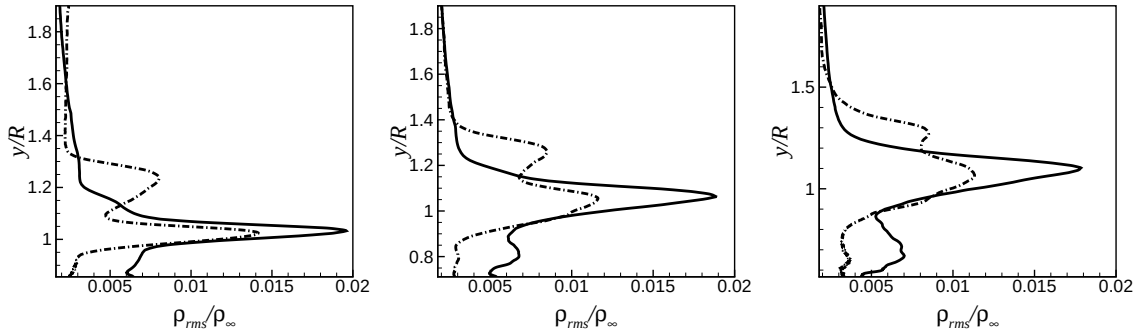

(a) $x = 3.0R$ (b) $x = 3.25R$ (c) $x = 3.5R$

Figure 10. Root-mean-square of density fluctuations for the baseline case and passive control case: ———, LES baseline; – · – · –, LES with passive control.

reduced optical distortions. This is consistent with the prediction of the model given by Gordeyev et al.[11]

The two-dimensional spatial correlations of OPD in the x'-y' plane is plotted in figure 11. It is observed that the shape of 2-D spatial correlation contours in the controlled case is similar to that in the baseline case. The correlation length in the controlled case is longer than that in the baseline case in both directions, indicating that the interaction between two shear layers has resulted in larger energetic flow scales.

IV. Conclusions

Large-eddy simulations of a compressible separated shear layer over a cylindrical turret with and without passive control devices in the upstream boundary layer have been performed. The control devices consist of long and thin pins as in the experimental configuration of Gordeyev et al.[11] Only one set of pin parameters have been considered at turret elevation angle of 120°. Comparison with the experimental data for the baseline case without pins shows overall agreement except for small discrepancies in the shear layer position and velocity fluctuation magnitude. Simulation of the passive-control case confirmed key experimental observations. A second shear layer above the main shear layer is observed, which reduces the turbulence intensity of the main shear layer and widens the turbulence region over the optical window. The optical calculation shows that optical distortions are reduced by 6% in magnitude, suggesting that this configuration is not very effective. The experiment of Gordeyev et al.[11] yielded a slight increase in optical distortions.

The simulation of flow control with pins is very challenging and considerable discrepancies with experimental data still exist because of the demanding grid resolution requirement imposed by the complex geometry and wide range of important flow scales, as well as uncertainties in boundary conditions and 3-D effect in the experiment. The discrepancies in the mean velocity and rms of velocity fluctuations between the simulation and experiment require further investigation. In particular, grid resolution in the wake of pins

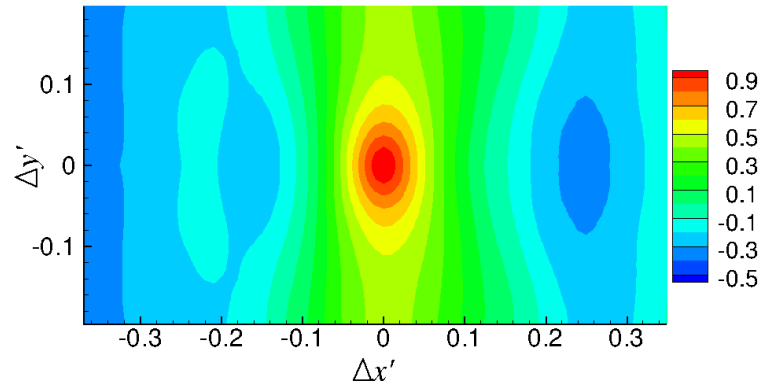

(a)

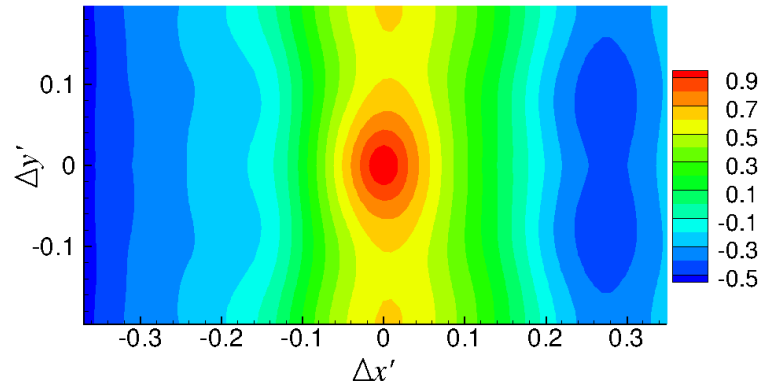

(b)

Figure 11. Spatial correlations of OPD in the x'-y' plane: (a) baseline case; (b) passive control case.

need to be carefully examined and improved in order to faithfully represent the energetic wake structures over a large distance, until they are past the optical window. Other issues, including boundary conditions and the 3-D effect in the experiment, should be examined as well.

Acknowledgments

This work was sponsored by the High Energy Laser Joint Technology Office (HEL-JTO) through AFOSR Grant FA 9550-07-1-0504. The U.S. Government is authorized to reproduce and distribute reprints for government purposes notwithstanding any copyright notation thereon. We wish to thank Mohammad Shoeybi of Stanford University for assistance with the LES code.

References

[1]Jumper, E. J. and Fitzgerald, E. J., "Recent Advances in Aero-Optics," *Progress in Aerospace Sciences*, Vol. 37, No. 3, 2001, pp. 299–339.

[2]Tromeur, E., Garnier, E., Sagaut, P. and Basdevant, C., "Large Eddy Simulation of Aero-Optical Effects in a Turbulent Boundary Layer," *Journal of Turbulence*, Vol. 4, 2003, pp. 1–22.

[3]Tromeur, E., Garnier, E. and Sagaut, P., "Large-Eddy Simulation of Aero-Optical Effects in a Spatially Developing Turbulent Boundary Layer," *Journal of Turbulence*, Vol. 7, 2006, pp. 1–28.

[4]Childs, R. E., "Prediction and Control of Turbulent Aero-optical Distortion Using Large Eddy Simulation," AIAA Paper 1993-2670.

[5]Visbal, M. R. and Rizzetta, D. P., "Effect of Flow Excitation on Aero-Optical Aberration," AIAA Paper 2008-1074.

[6]Mani, A., Wang, M. and Moin, P., "Statistical Description of Free-Space Propagation for Highly Aberrated Optical Beams," *Journal of Optical Society of America A*, Vol. 23, No. 12, 2006, pp. 3027–3035.

[7]Mani, A., Moin, P. and Wang, M., "Computational Study of Optical Distortions by Separated Shear Layers and Turbulent

Wakes," *Journal of Fluid Mechanics*, Vol. 625, 2009, pp. 273–298.

[8]Jones, M. I. and Bender, E. E., "CFD-Based Computer Simulation of Optical Turbulence Through Aircraft FLowfields and Wakes," AIAA Paper 2001-2798.

[9]Cress, J., Gordeyev, S., Jumper, E., Ng, T. T. and Cain, A. B., "Similarities and Differences in Aero-Optical Structure over Cylindrical and Hemispherical Turrets with a Flat Window", AIAA Paper 2007-0326.

[10]Gordeyev, S., Jumper, E., Ng, T. T. and Cain, A. B., "The Optical Environment of a Cylindrical Turret with a Flat Window and the Impact of Passive Control Devices," AIAA Paper 2005-4657.

[11]Gordeyev, S., Cress, J., Smith, A. and Jumper, E., "Improvement in Optical Environment over Turrets with Flat Window Using Passive Flow Control," AIAA Paper 2010-4492.

[12]Wang, K. and Wang, M., "Numerical Simulation of Aero-Optical Distortions by a Turbulent Boundary Layer and Separated Shear Layer," AIAA Paper 2009-4223.

[13]Morgan, P. E. and Visbal, M. R., "Large Eddy Simulation of Flow over a Flat-Window Cylindrical Turret with Passive Flow Control," AIAA Paper 2010-916.

[14]Shoeybi, M., Svard, M., Ham, F. E. and Moin, P., "An Adaptive Implicit-Explicit Scheme for the DNS and LES of Compressible Flows on Unstructured Grids," *Journal of Computational Physics*, Vol. 229, No. 17, pp. 5944–5965.

[15]Gladstone, J. H. and Dale T. P., " Researches on the Refraction, Dispersion, and Sensitivities of Liquids," *Philosophical Transactions of the Royal Society of London*, Vol. 153, 1863, pp. 317–343.

[16]Lund, T. S., Wu, X. and Squires, K., "Generation of Turbulent Inflow Data for Spatially-Developing Boundary Layer Simulations," *Journal of Computational Physics*, Vol. 140, No. 2, 1998, pp. 233–258.

[17]Sagaut, P., Garnier, E., Tromeur E., Larcheveque, L. and Labourasse, E., "Turbulent Inflow Conditions for Large-Eddy Simulation of Compressible Wall-Bounded Flows," *AIAA Journal*, Vol. 42, No. 3, 2004, pp. 469–477.

[18]Xu, S. and Martin, M. P., "Assessment of Inflow Boundary Conditions for Compressible Turbulent Boundary Layers," *Physics of Fluids*, Vol. 16, No. 7, 2004, pp. 2623–2639.

[19]Colonius, T., "Modeling Artificial Boundary Conditions for Compressible Flow," *Annual Review of Fluid Mechanics*, Vol. 36, 2004, pp. 315–345.

[20]Sutton, G.W., "Aero-Optical Foundations and Applications," *AIAA Journal*, Vol. 23, No. 10, 1985, pp. 1525–1537.